

Albert D. G. de Roos · Everardus J. J. van Zoelen
Alexander P. R. Theuvenet

Determination of gap junctional intercellular communication by capacitance measurements

Received: 27 July 1995/Received after revision: 2 October 1995/Accepted: 3 October 1995

Abstract Electrical coupling between cells is usually measured using the double patch-clamp technique with cell pairs. Here, a single patch-clamp technique that is not limited to cell pairs is described to determine electrical coupling between cells. Capacitance measurements in clusters of normal rat kidney (NRK) fibroblasts were used to study intercellular communication. In the whole-cell patch-clamp configuration capacitive transients were evoked by applying small voltage pulses. Total membrane capacitance was calculated from these capacitive transients after determination of access resistance, membrane conductance, and the decay constant of the transients, or alternatively by integrating the current transient. We found that in clusters of one to ten cells, membrane capacitance increased linearly with cell number, showing that the cells are electrically coupled. Membrane conductance of the cluster of cells also increased, as expected for cells that are well coupled. In subconfluent and confluent cultures, high membrane conductances together with large capacitive transients were observed, indicative of electrical coupling. Capacitance could only be determined qualitatively under these conditions, due to space clamp problems. In the presence of the gap junctional inhibitors halothane, heptanol or octanol, capacitance of all clusters of cells fell to single-cell levels, showing a complete uncoupling of the cells. The tumour promoter 12-*O*-tetradecanoylphorbol-13-acetate (TPA) also uncoupled the cells completely, within 10 min. We conclude that capacitance measurements can provide a useful tool to study changes in intercellular communication in clusters of cells.

Key words Intercellular communication · Gap junctions · Electrical coupling · Capacitance · Patch clamp · Whole cell

Introduction

Gap junctional intercellular communication plays an important role in many biological processes. Coupling between cells has, for instance, been implicated in the propagation of cardiac action potentials and contraction of smooth muscle [20], embryonic development [10], synchronization of hormone secretion in the pancreas [18], regulation of blood flow [4], and in the regulation of cell proliferation [13].

Intercellular communication through gap junctions is mediated by connexin proteins and can be modulated by several mechanisms. Elevation of the intracellular calcium concentration, intracellular acidification, and lipophilic substances such as heptanol, octanol, and halothane have been shown to reduce intercellular communication. Phosphorylation, stimulated by adenosine 3',5'-cyclic monophosphate (cAMP) or 12-*O*-tetradecanoylphorbol-13-acetate (TPA), also decreases coupling between cells (reviewed in [7]).

Several methods exist to study intercellular communication. Various biochemical techniques have been developed in which the transfer of a tracer molecule is followed. These techniques include dye transfer after scrape loading [5] or microinjection [23], fluorescence recovery after photobleaching [28], metabolic co-operation [30], and radioactive metabolite transfer [8]. Electrical communication in cell pairs can be measured using the double voltage-clamp technique with microelectrodes [21] or by determining the gap junctional conductance using the double whole-cell patch-clamp technique [16].

Although gap junctions allow transfer of molecules up to 1 kDa [19], molecules smaller than 1 kDa are

A. D. G. de Roos (✉) · E. J. J. van Zoelen · A. P. R. Theuvenet
Department of Cell Biology, University of Nijmegen,
Toernooiveld 1, 6525 ED Nijmegen, The Netherlands

not always transferred effectively and even transfer of molecules of the same size can be different [2, 27, 29]. Moreover, cells that are not dye coupled can still be electrically coupled [22, 25]. Differences in dye and electrical coupling may depend on the physical and chemical properties of the dye, and the type of connexin involved [2, 22, 25, 27]. Therefore, intercellular communication studied using biochemical techniques only shows whether the cells are coupled for the dye used and will not always give information about electrical coupling. On the other hand, measurement of electrical coupling using double voltage-clamp techniques is technically difficult because it requires the use of at least two electrodes. Theoretically, the double patch-clamp technique can be applied to multicellular preparations but mathematical analysis of the data obtained from those experiments is complicated. Therefore, this technique is mostly used to determine electrical coupling of isolated cell pairs only.

Here, we describe a simple single patch-clamp technique that is not limited to cell pairs to assay electrical intercellular communication. With increasing numbers of cells in a cluster, the total membrane surface, and thus the capacitance, will increase when the cells are electrically coupled. We used this principle to determine intercellular coupling in clusters of normal rat kidney (NRK) fibroblasts. NRK cells have been shown to be coupled biochemically [6, 11, 14] as well as electrically [14]. Using capacitance measurements, we show that clusters of NRK fibroblasts are electrically well coupled and may provide a good cell system to study electrical intercellular communication.

Materials and methods

Chemicals

Octanol, heptanol and halothane were from Aldrich (Steinheim, Germany), TPA was from Sigma (St. Louis, Mo., USA).

Cell culture

NRK fibroblasts (clone 49F) were seeded on plastic tissue culture dishes at a density of 10^3 to 10^4 cells per cm^2 in bicarbonate-buffered Dulbecco's modified Eagle's medium, supplemented with 10% bovine calf serum (HyClone Laboratories, Logan, VT, USA). Cells were cultured for 1–5 days at 37°C in 5% CO_2 . Single cells, small clusters of cells (two to ten cells), subconfluent and confluent cell cultures were used for patch-clamp studies. Cultures were called subconfluent when 30–50% of the culture dish was covered with cells and the patched cell was part of a cluster of at least 100 cells. At 10–15 min before using the cells for patch-clamp measurements, medium was replaced with a physiological salt solution, containing (in mM): 140 NaCl, 5 KCl, 2 CaCl_2 , 1 MgCl_2 , 10 Tris, 10 glucose, pH 7.4 at room temperature. In experiments in which the medium was changed, the cells were perfused at a rate of 1 ml/min in an incubation chamber with a volume of 0.6–0.8 ml.

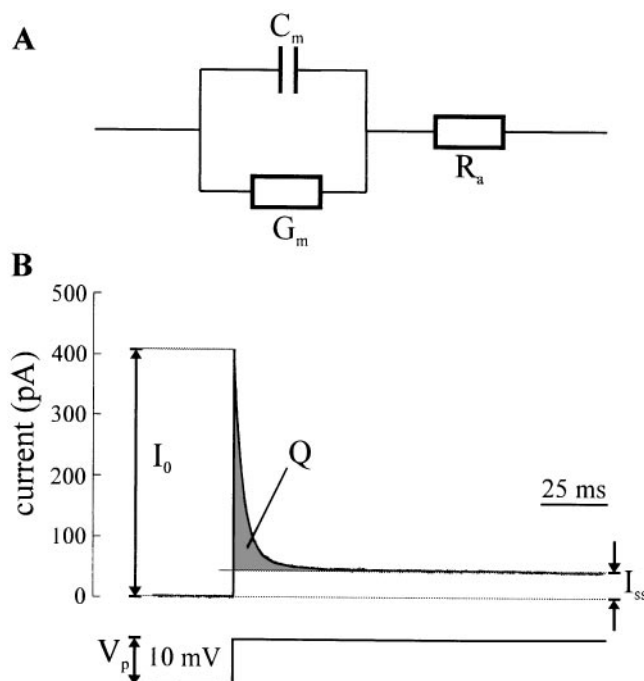
Whole-cell patch-clamp measurements

Conventional whole-cell patch-clamp methods were used. Patch pipettes were made from thin-walled glass (SG150T, Clarke Electromedical Instruments, Pangbourne, UK) using a two-stage pipette puller (L/M-3P-A, List Electronic, Darmstadt, Germany). Pipettes were carefully coated with Sylgard 184 (Dow Corning, Midland, Mich., USA). Pipettes were filled with a pipette solution [in mM: 25 NaCl, 120 KCl, 1 CaCl_2 , 1 MgCl_2 , 10 Tris, 3.5 ethylene glycol bis(aminoethylether)tetraacetic acid (EGTA), pH 7.4] and had resistances of 4–6 megaohms. Membrane currents were detected with an EPC-7 patch-clamp amplifier (List Electronic). In the cell-attached configuration, capacitance of the pipette was compensated. In the whole-cell configuration, however, capacitive transients of the cell membrane were not cancelled. In some experiments membrane potential was determined by switching to the current-clamp mode. Voltage-clamp protocols and data acquisition were performed using CED software in conjunction with a CED 1401 interface (Cambridge Electronic Design, Cambridge, UK). Data were filtered at 5 kHz, sampled at 12.5 kHz, and stored on hard disk for subsequent analysis.

Theoretical background

Determination of capacitance and membrane conductance were performed according to the method described by Lindau and Neher [12]. Figure 1A shows the minimal equivalent circuit of the whole-cell patch-clamp configuration. The cell membrane is characterized by the parallel combination of the membrane capacitance, C_m and

Fig. 1A Minimal equivalent circuit of the whole-cell patch-clamp technique. The cell membrane is represented by a capacitance C_m and a resistance R_m . The resistance between the pipette and the cell is indicated as the access resistance R_a . Seal resistance is assumed to be perfect and capacitance of the pipette assumed to be cancelled by the patch-clamp amplifier. **B** Current transient of a model cell as a result of a short voltage pulse (V_p) delivered through the pipette. I_0 is peak current at $t = 0$. Current will decay exponentially, and I_{ss} is the steady-state current after capacitor (i.e. membrane) has been charged. The area under the transient (Q) represents the charge accumulated on the membrane



the membrane conductance, G_m . The access resistance, R_a , of the pipette tip is in series with C_m and G_m . Figure 1B shows the current response to a voltage step delivered through the pipette (V_p). From this current response, values for the current at $t = 0$ (I_0), the steady-state current (I_{ss}), and the decay constant of transient (τ) can be obtained. The circuit parameters R_a , G_m and C_m can be related to these parameters through the following equations [12].

$$R_a = V_p / I_0 \quad (1)$$

$$G_m = I_{ss} / (V_p - R_a \cdot I_{ss}) \quad (2)$$

$$C_m = \tau \cdot [(1/R_a) + G_m] \quad (3)$$

In this minimal equivalent circuit of the whole-cell patch-clamp configuration, G_m is considered to be of pure ohmic behaviour. Since seal resistances were at least 20 G Ω , capacitance error will be less than 0.1% [12]. The area under the transient represents the total charge accumulated on the membrane [9]. Capacitance can be calculated by dividing the total charge (Q) by the applied voltage.

Data analysis

Capacitive current transients were obtained by applying a 10-mV voltage pulse. Capacitive transients were fit to a single exponential function using Bio-Patch software (Bio-Logic, France). The first three or four data points (about 0.3 ms) were neglected because they represent filter artefacts. When clusters of less than ten cells were used, all transients could be fit to a single exponential function, and I_0 , I_{ss} and τ were obtained from this fit. By insertion in Eqs. 1–3 R_a , G_m , and C_m were calculated. By integrating the current transient using Bio-Patch software, the accumulated charge Q (Fig. 1B) could be determined and C_m was obtained by dividing Q by V_p . In subconfluent and confluent cultures, data could no longer be fit to a single exponential. In these cases, I_0 was determined from a fit from the first section of the data, I_{ss} was measured from the raw data, and only R_a and G_m were calculated.

Results

NRK fibroblasts were patched in the whole-cell patch-clamp configuration and small (10 mV) voltage pulses were applied. In Fig. 2, the resulting current transient is shown in small clusters of cells (up to ten cells), and in subconfluent and confluent cell cultures. In patched single cells, the current transient was characterized by a small decay constant and a low steady-state current. With increasing cluster size, decay constants became larger and also steady-state current increased. Average decay constants were 0.51 ± 0.36 ms for single cells, and 5.31 ± 1.44 ms for clusters of ten cells. The average steady-state current values ranged from 1.05 ± 0.36 pA in single cells to 11.39 ± 4.82 pA in clusters of ten cells. Peak currents represent the access resistance of the pipette tip (Eq. 1) and are not related to cluster size. When subconfluent and confluent cultures were used, decay constants became even larger and very large steady-state currents became apparent. Increasing steady-state currents, at equal access resistances, indicate increasing membrane conductance, while increasing decay constants suggest an increasing capacitance. Thus, with increasing cluster size, the current transients indicated that membrane conductance and capacitance of the cluster of cells increased. This implied that the cells were electrically coupled.

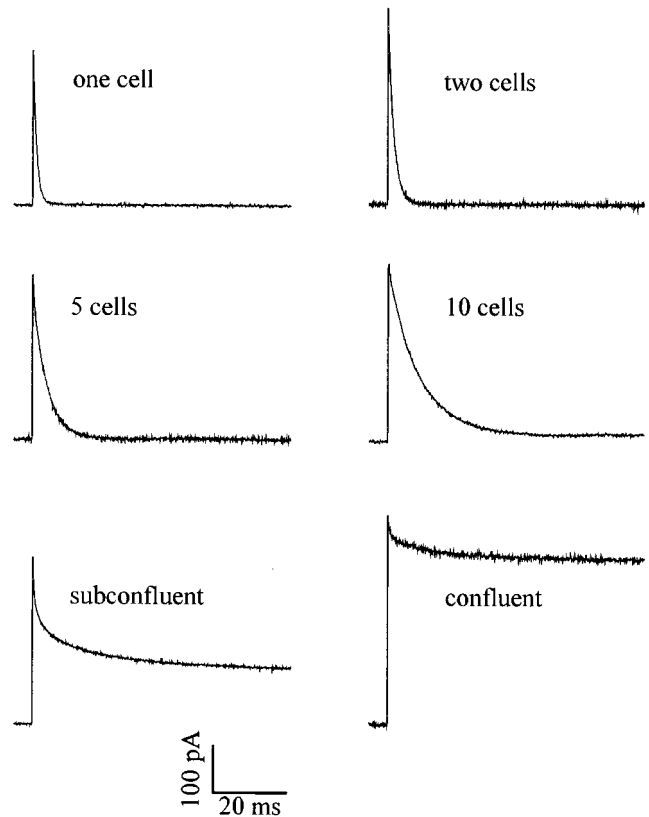


Fig. 2 Current response to a voltage pulse in normal rat kidney (NRK) cells. One cell of a cluster of cells was patched in the whole-cell configuration and a voltage pulse of 10 mV was given. Pipette capacitance was cancelled and transients represent capacitive transients of the cell membrane

Since decay constants are related to membrane capacitance, membrane capacitance was calculated from the evoked capacitive transients in clusters of up to ten cells. The capacitance was calculated after determination of access resistance, membrane conductance and decay constant (Fig. 3A), and alternatively through integration of the current transient (Fig. 3B), as described in Materials and methods. Single-cell capacitance was about 30 pS, while capacitance of a cluster of ten cells was about 300 pS. Figure 3A, B shows that capacitance increased linearly with cell number indicating electrical coupling. Figure 3C shows that both methods to determine capacitance yielded the same results, indicating that the variation in membrane capacitance at a specific cell number is not the result of variation in the method used to determine membrane capacitance, but represents an actual variation in the capacitance of the clusters of cells. This is most likely due to a variation in cell size.

With larger clusters (more than ten cells), decay constants could not be determined anymore, because the transients could not be fit with a single exponential, probably due to space clamp problems. These space clamp problems arise from the fact that the cytoplasm as well as the gap junctions have a certain resistance.

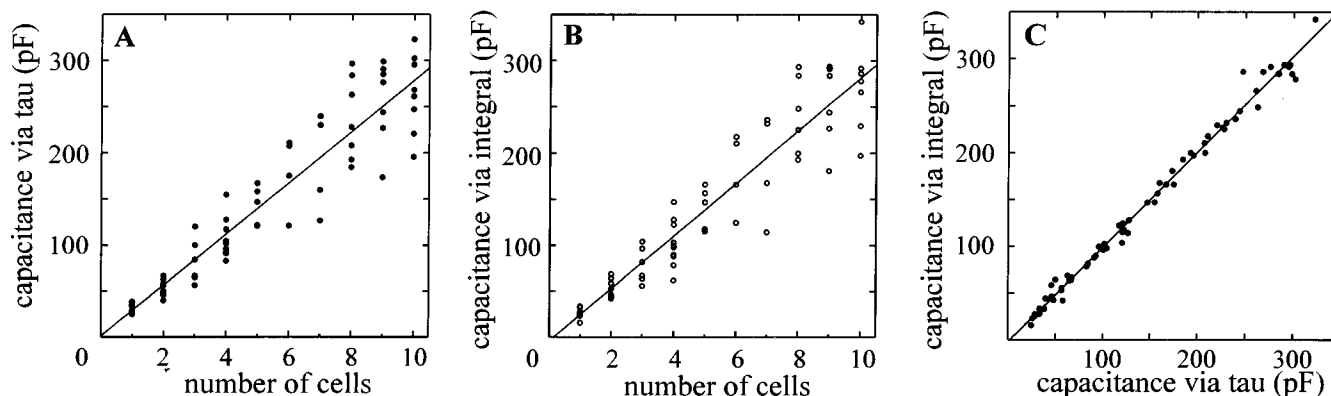


Fig. 3A–C Capacitance as a function of cell number. **A** Capacitance was determined after calculation of R_a , G_m and decay constant of capacitive current transients. **B** The integral of current transient was used to determine capacitance. **C** Capacitance calculated via the integral plotted against capacitance calculated via decay constant (τ), R_a and G_m . Each data point represents the value of an individual measurement at the indicated cell number

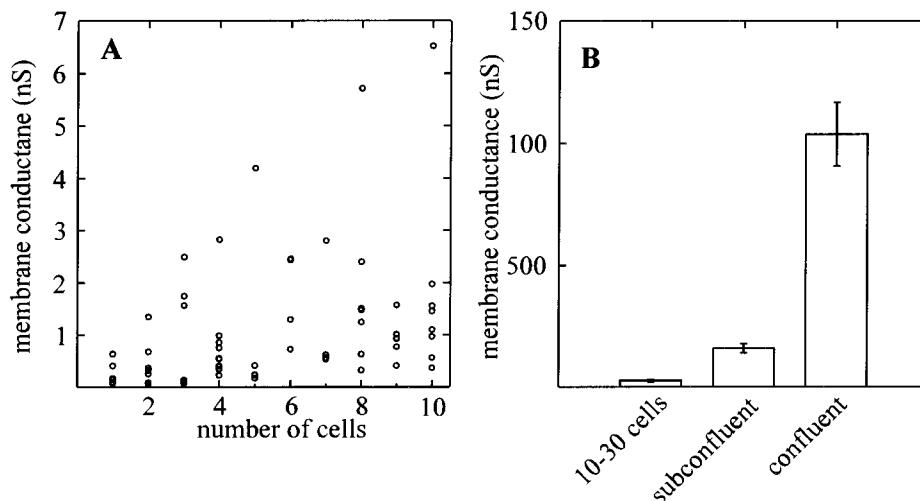
These resistances cause the voltage to drop and after a certain distance, voltage will be zero [1]. Because of these space clamp limitations, voltage will no longer be uniformly distributed and the monolayer can only be partly voltage-clamped.

In electrically coupled cells, it is expected that total membrane conductance will also increase with cell number. The steady state currents in Fig. 2 already suggested that membrane conductance increased with increasing cell numbers. Figure 4 shows the membrane conductance as a function of cell number. Membrane conductance was calculated from the access resistance and the steady-state currents (Eq. 2). From one to ten cells, membrane conductance increased, but variation in membrane conductance also increased (Fig. 4A). Membrane resistance of single cells was in the gigaohm range, but resistance of the membrane was only a few megaohms in confluent cells. This also showed that cells were electrically coupled. From the average num-

bers in Fig 4A no clear linear relation could be detected between membrane conductance and cell number, in contrast to membrane capacitance and cell number. A linear relation could be obscured by a large variation in membrane conductance in single cells, which could result from a variation in channel density. It is also possible that channel activity, and thereby membrane conductance, is a function of cell number and in that case, there does not have to be a linear relation. When we compared larger clusters of cells (10–30 cells) with subconfluent and confluent cells, membrane conductance increased dramatically (Fig. 4B). This increase suggests that coupling is maintained at high cell densities. Despite space clamp problems that probably occurred, the difference between subconfluent and confluent cells could be clearly seen. However, the observed membrane conductance will not be the conductance of the whole monolayer, because only part of the monolayer will be voltage-clamped.

We also tested the known gap junctional blockers halothane, heptanol and octanol on the ability to block gap junctional communication in NRK cells by determining their effect on evoked capacitive transients. Figure 5 shows the effect of exposure of confluent, subconfluent and single cells to halothane (1.5 mM). Within seconds after addition of halothane to the bath,

Fig. 4A, B G_m as a function of cell number. **A** G_m of clusters of one to ten cells. Data points represent individual measurements. **B**. Membrane conductance in clusters of 10–30, subconfluent and confluent cells. *Errors bars* represent SEM values. G_m is the reciprocal of R_m



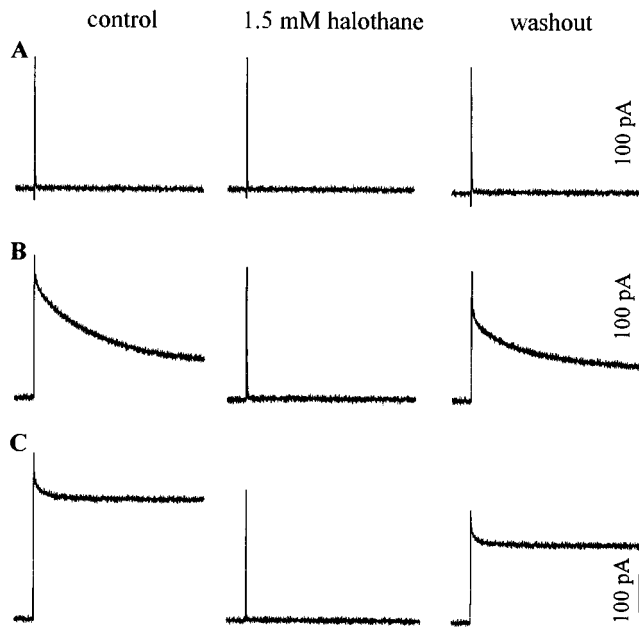


Fig. 5A–C The effect of the uncoupler halothane on capacitive current transient in NRK cells. **A** Single, **B** subconfluent and **C** confluent cells were treated with 1.5 mM halothane. *Left*: control current transients, *middle*: after treatment with halothane, *right*: after evaporation of halothane (about 5 min after addition)

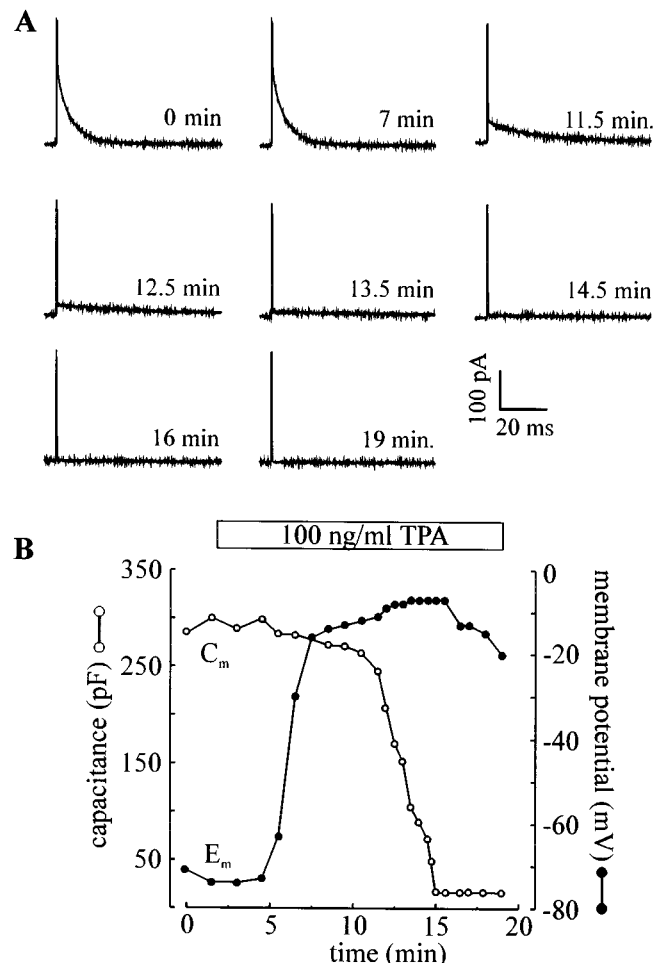
the decay constant and steady-state current of the capacitive transient fell to levels similar to that of single cells. This shows that halothane treatment results in complete functional uncoupling of the cells. Figure 5 also shows that after evaporation of halothane, coupling was re-established. Similar results (not shown) were obtained with heptanol (1.5 mM) and octanol (1.5 mM). These results show that the electrical communication in NRK cells is mediated through gap junctions and that capacitance measurements can be used to study modulation of this communication.

The phorbol ester TPA was used to follow a more physiological approach to modulate gap junctions. Activation of protein kinase C by TPA [7, 15] has been shown to block gap junctions by a phosphorylation of connexin. Figure 6A shows the capacitive transients of a cluster of 11 cells after treatment with 100 ng/ml TPA. After 5 min of TPA treatment the transient was still the same as in the control, but after 10 min the shape of the transient changed. First, the area under the curve became smaller, indicating a reduced capacitance. Second, the decay constant became larger. After 13 min of TPA treatment, both the area under the transient and the decay constant reached single-cell levels. We interpret these data as follows. When gap junctions are partially blocked, resistance between cells becomes larger. Therefore, the decay constant, which is equal to the product of the total resistance (R_a and $1/G_m$) and the capacitance, (from Eq. 3) becomes larger. The reduced area under the curve, i.e. the accumulated charge, decreases because the higher resistance between

cells prevents charging of all cells in the cluster. When the gap junctions are not totally blocked by TPA, the current transient represents the fast charging of the patched cell, and the slow charging of the rest of the cluster with much larger decay constants. The small decay constant at partial TPA block (0.10 ms) was similar to the decay constant at maximal TPA block (0.11 ms). Moreover, the capacitance calculated from an exponential fit of this fast part of the transient yielded a value comparable to those measured in single cells. Finally, when the gap junctions are totally blocked, the resistance between cells is very high, and only the capacitance of a single cell can be measured.

Figure 6B shows the calculated capacitance of the cluster of 11 cells in response to TPA treatment. Capacitance fell from a value of 300 pF, characteristic for a cluster of 11 cells, to a capacitance of 20 pF, characteristic for a single cell. No stepwise decreases in capacitance were observed. The figure shows the capac-

Fig. 6A, B The effect of 12-*O*-tetradecanoylphorbol-13-acetate (TPA) on coupling and membrane potential. **A** Capacitive current transients are shown in a cluster of 11 cells at different times after perfusion of 100 ng/ml TPA. **B** Corresponding calculated capacitance and membrane potential. Capacitance was calculated via integration of the capacitive current transients. Membrane potential was determined in the current-clamp mode



itance calculated from the integrated transient, because the data could not be fit with a single exponential when TPA block was not complete. Control values and values at complete block calculated through the decay constant yielded similar results to those calculated via the integral of the current. From the decreased membrane capacitance values, one cannot deduce the number of coupled cells, but the values will only give an estimate as to what extent coupling is reduced. Membrane potential also dropped (Fig. 6B) after addition of TPA from an initial value of -70 mV to -5 mV. It has been reported that transmembrane potential can affect intercellular coupling [16]. Clearly, membrane depolarization preceded the decrease in capacitance, and is, therefore, not directly related to the change in capacitance. We cannot exclude the possibility, however, that membrane depolarization is a prerequisite for uncoupling.

Discussion

Several methods have been described to measure gap junctional communication. These include techniques to assay biochemical communication, in which the diffusion of tracer molecules was followed, and electrical communication, using voltage-clamp techniques. Biochemical communication may not be a good measure for electrical coupling. In several instances electrical coupling of cells has been demonstrated in the absence of dye coupling [22, 25, 29]. Also, a reduction in gap junctional coupling may abolish transfer of, for instance, fluorescent dyes, but remaining electrical coupling may be sufficient to transduce electrical signals [2, 27]. Measurements of electrical communication between cells are usually performed using double voltage-clamp techniques on cell pairs, but these measurements have been hampered by the fact that they are technically difficult and require two patch-clamp setups. The mathematical analysis when clusters of cells are used is complex and requires cable analysis [1].

Here, we describe a simple single patch-clamp technique, that is not limited to cell pairs, to study electrical intercellular communication. The advantage of the technique presented here, is the fact that only one patch-clamp electrode is needed to assay electrical communication, in contrast to the double voltage-clamp techniques. The capacitance of clusters of cells was measured to determine gap junctional coupling. Since the membrane acts as a capacitor, capacitance is directly related to membrane area and therefore cell size. The specific membrane capacitance is about $1 \mu\text{F}/\text{cm}^2$ [9]. In NRK cells, capacitance increased linearly with cell number, showing that capacitance measurements can be used to assess electrical coupling in these cells. When large cells or clusters of cells are voltage-clamped, measurements will be limited by the space

clamp phenomenon: applied voltage via the pipette will gradually decrease in space, due to the resistance of the cytosol and the gap junctions [1]. The fact that in small clusters of cells, capacitance increased linearly with cell number, indicates that gap junctional resistance is so low that in these small clusters of cells no space clamp problems occur. Space clamp problems will result in a non-linear relation between capacitance and membrane area or capacitance. Since NRK cells in culture tend to move and spread out, it is hard to find nicely aggregated clusters of more than 15 cells. Therefore, we could not determine precisely at what cluster size the linear relation between cell number and capacitance was lost. However, current transients could be fit by a single exponential in clusters of 30 cells, indicating no significant space clamp problems.

In subconfluent and confluent cell cultures, current transients could no longer be fit by a single exponential. In these cases, we used membrane conductance as an indication for coupling. In electrically coupled cells membrane conductance of neighbouring cells will be measured. We observed an increase in total membrane conductance as a function of cell number in NRK cells, indicating electrical coupling of the cells. Here, a clear linear relation could not be found, in contrast with the capacitance measurements. Although capacitance is a direct measure of membrane area, membrane conductance is determined by the number and the open probability of ion channels in the membrane. These parameters can be influenced by coupling or cell density and therefore, membrane conductance does not have to be directly related to cell number in coupled cells.

We also showed that capacitance measurements can be used to measure a reduction in gap junctional intercellular communication. Gap junctions can be blocked by lipophilic agents such as heptanol, octanol or halothane [3, 24], and by activation of protein kinase C using TPA [15, 26, 30]. Here, we showed that lipophilic agents and TPA inhibit intercellular communication in NRK cells, which demonstrates that electrical coupling is mediated through gap junctions.

Capacitance measurements can show uncoupling in a cluster of cells, although no absolute values of coupling can be obtained. Since NRK cells are well coupled, a complete uncoupling can be easily shown by a capacitance value that is similar to single-cell values. Partial uncoupling of a cluster of cells can mean that some of the cells uncouple from the other cells that remain coupled. In these cases, a decreased capacitance will be measured, namely the capacitance value of the cells that remain electrically coupled to the patched cell. In these cases a stepwise decrease in capacitance can be expected. Since differences in capacitance of clusters of cells of different cell number could be determined (Fig. 3), it should be possible to measure a stepwise decrease in capacitance resulting from the

uncoupling of certain cells in a cluster of cells. However, in our experiments stepwise decreases were never seen.

A partial uncoupling will also be seen, when the gap junctional conductances of all the cells is reduced. A decrease in gap junctional conductance will result in a larger decay constant (see Eq. 3). This will lead to a lower measured membrane capacitance, except when this conductance decrease does not prevent complete charging of the cluster of cells. However, also a decrease in membrane conductance will cause a larger decay constant (Eq. 3), but in these cases capacitance will always stay the same. In our experiments, partial uncoupling by TPA resulted in a larger decay constant (Fig. 6), together with a decrease in capacitance. Calculated capacitance would not have been decreased if TPA decreased membrane conductance, but we cannot exclude the possibility that the increased decay constant is partly due to a decreased membrane conductance. In conclusion, capacitance measurements can give qualitative information about modulation of coupling, but no absolute values of uncoupling can be obtained.

NRK cells have been shown to be coupled electrically using microelectrodes and biochemically using dye microinjection [14], dye transfer with a preloading technique [6] or fluorescence-activated cell sorting [11]. Measurement of biochemical coupling appears to depend on the dye used, because in some experiments only a limited coupling was observed in NRK cells [31]. However, these conflicting data on gap junctional coupling of NRK cells might be related to possible differences in growth state of the cells used in these studies. Recently, namely, a cell-state-dependent modulation of gap junctional communication in NRK cells has been reported [17].

Capacitance measurements may provide a useful tool to study modulation of electrical intercellular communication in NRK cells. It has been shown that growth factors like epidermal growth factor and platelet-derived growth factor inhibited gap junctional communication in NRK cells [14]. Intracellular pH, phosphorylation and the intracellular calcium concentration can affect intercellular coupling in cells [7]. We are currently investigating how these components of mitogenic/transforming pathways may modulate gap junctional communication in NRK fibroblasts.

Our observation that capacitance of small clusters of NRK cells increased linearly with cell number showed that, electrically, small clusters of cells behave like a functional syncytium. In larger clusters and subconfluent and confluent cells, capacitance could not be determined quantitatively anymore, but large capacitive transients together with high membrane conductances suggested that many, if not all, cells in a monolayer were coupled. Strong electrical coupling implicates that the membrane of the whole monolayer of cells is isopotential. This has also been shown in cultured guinea-pig coronary endothelial cells [4]. Like

NRK cells, monolayers of these cells were also characterized by low input resistances. In strongly coupled cells, measurement of membrane potential in monolayers will actually represent the average membrane potential of many cells. In coupled cells, de- or hyperpolarizations of the membrane will be also uniformly distributed. We recently showed that agonists, such as bradykinin and prostaglandin $F_{2\alpha}$ depolarize NRK cells (A.D.G. de Roos et al., submitted). A function of electrical coupling between NRK cells may be the transduction of de- or hyperpolarizations and changes in gap junctional coupling may affect this transduction. Moreover, membrane potential is much more stable in subconfluent and confluent cells than in small clusters of cells (A. D. G. de Roos et al., unpublished). Therefore, another function of electrical coupling might be stabilization of the membrane potential.

In conclusion, capacitance measurements using the single whole-cell patch-clamp technique provide a useful tool to determine intercellular electrical coupling in clusters of cells. Since NRK cells are electrically well coupled, they provide an excellent model system to study control of intercellular communication.

Acknowledgements We would like to thank Dr. Maarten Kansen, department of Biochemistry, University of Nijmegen, for critically reading the manuscript and Dr. Martin Rook, department of Medical Physiology, University of Utrecht, for helpful discussions. This research was funded by the Netherlands foundation for life sciences.

References

1. Armstrong CM, Gilly WF (1992) Access resistance and space clamp problems associated with whole-cell patch clamping. *Methods Enzymol* 207:100–122
2. Brissette JL, Kumar NM, Gilula NB, Hall JE, Dotto GP (1994) Switch in gap junction protein expression is associated with selective changes in junctional permeability during keratinocyte differentiation. *Proc Natl Acad Sci USA* 91:6453–6457
3. Burt JM, Spray DC (1989) Volatile anesthetics block intercellular communication between neonatal rat myocardial cells. *Circ Res* 65:829–837
4. Daut J, Mehrke G, Nees S, Newman WH (1988) Passive electrical properties and electrogenic sodium transport of cultured guinea-pig coronary endothelial cells. *J Physiol (Lond)* 402:237–254
5. El-Fouley MH, Trosko JE, Chang CC (1987) A rapid and simple technique to study gap junctional intercellular communication. *Exp Cell Res* 168:422–430
6. Goldberg GS, Bechberger JF, Naus CCG (1995) Scrape loading and dye transfer. A pre-loading method of evaluating gap junctional communication by fluorescent dye transfer. *Bio-techniques* 18:490–497
7. Holder JW, Elmore E, Barrett JC (1993) Gap junction function and cancer. *Cancer Res* 53:3475–3485
8. Hooper ML (1982) Metabolic co-operation between mammalian cells in culture. *Biochim Biophys Acta* 651:85–103
9. Kado RT (1993) Membrane area and electrical capacitance. *Methods Enzymol* 221:273–299
10. Kalimi GH, Lo CW (1988) Communicating compartments in the gastrulating mouse embryo. *J Cell Biol* 107:241–255

11. Kiang DT, Kollander R, Lin HH, LaVilla S, Atkinson MM (1994) Measurement of gap junctional communication by fluorescence activated cell sorting. *In Vitro Cell Dev Biol* 30A: 796–802
12. Lindau M, Neher E (1988) Patch-clamp techniques for time-resolved capacitance measurements in single cells. *Pflügers Arch* 411:137–146
13. Loewenstein WR (1981) Junctional intercellular communication: the cell-to-cell membrane channel. *Physiol Rev* 61: 829–913
14. Maldonado PE, Rose B, Loewenstein WR (1988) Growth factors modulate junctional cell-to-cell communication. *J Membr Biol* 106:203–210 ((203–210))
15. Murray AW, Fitzgerald DJ (1979) Tumor promoters inhibit metabolic cooperation in cocultures of epidermal and 3T3 cells. *Biochem Biophys Res Commun* 91:395–401
16. Neyton J, Trautmann A (1985) Single-channel currents of an intercellular junction. *Nature* 317:331–335
17. Paulson AF, Johnson RG, Atkinson MM (1994) Intercellular communication is reduced by TPA and Ki-ras p21 in quiescent, but not proliferating, NRK cells. *Exp Cell Res* 213:64–70
18. Santos RM, Rosario LM, Nadal A, Garcia-Sancho J, Soria B, Valdeolmillos M (1991) Widespread synchronous $[Ca^{2+}]_i$ oscillations due to bursting electrical activity in single pancreatic islets. *Pflügers Arch* 418:417–422
19. Simpson I, Rose B, Loewenstein WR (1977) Size limit of molecules permeating the junctional membrane channels. *Science* 195:294–296
20. Spray DC, Bennett MVL (1985) Physiology and pharmacology of gap junctions. *Annu Rev Physiol* 47:281–303
21. Spray DC, Harris AL, Bennett MVL (1981) Equilibrium properties of a voltage-dependent junctional conductance. *J Gen Physiol* 77:77–93
22. Steinberg TH, Civitelli R, Geist ST, Robertson AJ, Hick E, Veenstra RD, Wang H-Z, Warlow PM, Westphale EM, Laing JG, Beyer EC (1994) Connexin43 and connexin45 form gap junctions with different molecular permeabilities in osteoblastic cells. *EMBO J* 13:744–750
23. Stewart WW (1978) Gap junctional connections between cells as revealed by dye-coupling with a highly fluorescent naphthalimide tracer. *Cell* 14:741–759
24. Takens-Kwak BR, Jongsma HJ, Rook MB, van Ginneken ACG (1992) Mechanisms of heptanol induced uncoupling of cardiac junctions: a perforated patch clamp study. *Am J Physiol* 262:C1531–C1538
25. Traub O, Eckert R, Lichtenberg-Fraté H, Elfgang C, Bastide B, Scheidtmann KH, Hülser DF, Willecke K (1994) Immunohistochemical and electrophysiological characterization of murine connexin40 and -43 in mouse tissues and transfected human cells. *Eur J Cell Biol* 64:101–112
26. Trosko JE, Chang CC, Madhakar BV, Klaunig JE (1990) Chemical, oncogene and growth factor inhibition of gap junctional intercellular communication: an integrative hypothesis of carcinogenesis. *Pathobiology* 58:265–278
27. Veenstra RD, Wang H-Z, Beyer EC, Ramanan SV, Brink PR (1994) Connexin 37 forms high conductance gap junction channels with subconductance state activity and selective dye and ionic permeabilities. *Biophys J* 66:1915–1928
28. Wade MH, Trosko JE, Schindler MA (1986) A fluorescent photobleaching assay of gap junction mediated communication between human cells. *Science* 232:525–528
29. von der Weid PY, Bény J-L (1993) Simultaneous oscillations in the membrane potential of pig coronary artery endothelial and smooth muscle cells. *J Physiol (Lond)* 471:13–24
30. Yotti LP, Chang CC, Trosko JE (1979) Elimination of metabolic cooperation in Chinese hamster cells by a tumor promoter. *Science* 206:1089–1091
31. van Zoelen EJJ, Tertoolen LGJ (1991) Transforming growth factor- β enhances the extent of intercellular communication between normal rat kidney cells. *J Biol Chem* 266:12075–12081